Investigating the geochemical model for molybdenum mineralization in the JEB Tailings Management Facility at McClean Lake, Saskatchewan: An X-ray absorption spectroscopy study

Peter E. R. Blanchard, John R. Hayes, Andrew P. Grosvenor*

Department of Chemistry, University of Saskatchewan, Saskatoon, SK, S7N 5C9

John Rowson, Kebbi Hughes, Caitlin Brown

AREVA Resources Canada, Saskatoon, SK, S7K 3X5

*Author to whom correspondence should be addressed
E-mail: andrew.grosvenor@usask.ca
Phone: (306) 966-4660
Fax: (306) 966-4730

Abstract

The geochemical model for Mo mineralization in the JEB Tailings Management Facility (JEB TMF), operated by AREVA Resources Canada at McClean Lake, Saskatchewan, was investigated using X-ray Absorption Near-Edge Spectroscopy (XANES), an elemental-specific technique that is sensitive to low elemental concentrations. Twenty five samples collected during the 2013 sampling campaign from various locations and depths in the TMF were analyzed by XANES. Mo K-edge XANES analysis indicated that the tailings consisted primarily of Mo^{6+} species: powellite ($CaMoO_4$), ferrimolybdite ($Fe_2(MoO_4)_3 \bullet 8H_2O$), and molybdate adsorbed on ferrihydrite ($Fe(OH)_3 - MoO_4$). A minor concentration of a Mo^{4+} species in the form of molybdenite (MoS_2) was also present. Changes in the Mo mineralization over time were inferred by comparing the relative amounts of the Mo species in the tailings to the independently measured aqueous Mo pore water concentration. It was found that ferrimolybdite and molybdate adsorbed on ferrihydrite initially dissolves in the TMF and precipitates as powellite.

Introduction

The JEB Tailings Management Facility (JEB TMF) plays a central role in reducing the environmental impact of AREVA Resources Canada's (AREVA) uranium ore mining operations in Northern Saskatchewan. The geochemistry of the tailings management system is designed to reduce the migration of water-soluble elements that co-mineralize with U ore (i.e. As, Ni, Mo, and Se) by promoting the formation of mineral species.[1] However, when initially added to the tailings, the concentration of the solutes are generally out of equilibrium with the desired minerals, requiring a long period of time to reach their respective mineralogical end point.[1] As such, predicting and controlling the long-term mineralization in the TMF is essential to prevent pollutant elements from contaminating the surrounding environment.

AREVA has been investigating the long-term mineralization of elements such as As and Ni in the TMF for many years.[2-4] $As^{5+}_{(aq)}$ concentrations are well controlled (< 1 mg/L) because of the co-precipitation of $Fe^{3+}_{(aq)}$ and $As^{5+}_{(aq)}$ as poorly crystalline scorodite ($FeAsO_4 \bullet 8H_2O$) because of the excess Fe in the TMF.[2-4] Likewise, $Ni^{2+}_{(aq)}$ concentrations are controlled by the adsorption of $Ni^{2+}_{(aq)}$ on ferrihydrite ($Fe(OH)_3$).[3] There has been comparatively fewer studies of how Mo mineralization in the TMF. The primary Mo-bearing mineral in the ore is molybdenite (MoS_2),[5] which is oxidized to water-soluble molybdate ($[MoO_4]^{2-}_{(aq)}$) when leeching (pH ~1) the uranium ore at the JEB uranium mill.[6] During the tailings preparation process, the waste solid and solution are mixed with ferric sulfate ($Fe_2(SO_4)_3$). Although intended to control the release of arsenic in the TMF, $Fe^{3+}_{(aq)}$ will also co-precipitate with $[MoO_4]^{2-}_{(aq)}$ to form ferrimolybdite ($Fe_2(MoO_4)_3 \bullet 8H_2O$) and molybdate adsorbed on ferrihydrite ($Fe(OH)_3 - MoO_4$) as the pH is raised to 4.[1,6] The pH is then raised to 7-8 prior to adding the tailings slurry to the TMF. $[MoO_4]^{2-}_{(aq)}$ is predicted to be present in the TMF because ferrimolybdite and molybdate

adsorbed on ferrihydrite are soluble under the near-neutral conditions of the TMF. Coincidentally, the TMF is saturated with gypsum ($CaSO_4 \bullet 2H_2O$) because of the addition of sulfuric acid (H_2SO_4) and lime (CaO) during the milling process, resulting in high concentrations of $Ca^{2+}_{(aq)}$ (500 mg/L) and $[SO_4]^{2-}_{(aq)}$ (2800 mg/L) throughout the pore water of the TMF. Thermodynamic calculations predict that the strongly oxidizing conditions of the TMF, with an Eh of +290 mV and a dissolved O^{2-} concentration of 5-7 mg/L, would promote the co-precipitation of $Ca^{2+}_{(aq)}$ and $[MoO_4]^{2-}_{(aq)}$ as powellite ($CaMoO_4$).[6] The overall geochemical model for the formation of powellite can be described by the following reaction:

$$CaSO_4 \bullet 2H_2O_{(s)} + [MoO_4]^{2-}_{(aq)} \rightarrow CaMoO_{4(s)} + [SO_4]^{2-}_{(aq)} + 2H_2O_{(l)} \quad (1)$$

X-ray absorption near-edge spectroscopy (XANES) and X-ray diffraction (XRD) analysis of tailings samples from the JEB TMF collected during the 2008 sampling campaign confirmed the presence of powellite in the TMF.[7] However, it was not possible to determine if the predicted mineralogical end-point of powellite is correct as only six samples were analysed. Powellite was also observed in a related XANES study on the Mo speciation in the Deilmann Tailings Management Facility (DTMF) operated by the Cameco Corporation.[5] Given the environmental implications, it is important to confirm that the geochemical model for controlling the release of Mo in JEB TMF is correct. XANES was used to identify and quantify the concentrations of the various Mo species in the TMF by analyzing tailings samples collected during the 2013 sampling campaign. XANES is a powerful analytical technique for studying environmental samples because it can be used to identify low concentrations of chemical species present in heterogeneous samples. Twenty five samples were studied, representative of the total depth of the tailings from two bore holes in the TMF. The sampling depth itself correlates with the age of the tailings due to the settled nature of the TMF. Therefore, the mineralization of Mo

62 in the TMF can be inferred by comparing the concentration of the various Mo species in the
63 tailings solids to the concentration of aqueous Mo in the tailings pore water. This study verified
64 the existing geochemical model and confirmed that powellite controls the aqueous Mo pore
65 water concentration in the TMF.

66 **Experimental**

67 **Tailings sample description and analysis**

68 The twenty-five samples analysed in this study were collected from two bore hole
69 locations during the 2013 sampling campaign of the JEB TMF. Fourteen of the samples were
70 collected from a bore hole located at the centre of the TMF (TMF13-01) while eleven of the
71 samples were collected from a periphery bore hole (TMF13-03) located 55 m from the central
72 bore hole. The tailings are placed in the TMF using a floating barge and tremie piping system.
73 While the design minimizes particle size segregation at the point of placement, it does not
74 eliminate it. Consequently, with respect to particle size distribution, the tailings solids in the
75 TMF are not homogenous. The central bore hole possesses a significantly coarser particle size
76 distribution than the peripheral bore hole. Tailings solids from the central bore hole can contain
77 large grains of primary Mo mineralization (molybdenite; MoS_2) that were too large to be fully
78 oxidized in the uranium mill process.

79 The samples were collected in approximately 3 m intervals using a Gregory-type piston
80 sampler by engineers from AREVA Resources Canada's Safety, Health, Environment, and
81 Quality (SHEQ) department. Material at the end of the sampler was discarded due to exposure
82 to air. The pore water was collected by hydraulically pressing the samples and analyzed using
83 inductively coupled plasma-mass spectrometry (ICP-MS) analysis to determine the aqueous Mo
84 pore water concentration. The Mo pore water concentration was found to vary from 1.25 – 44.20

mg/L. Solid tailings samples were nitrogen-purged, vacuumed-sealed, and stored in a freezer (~5 ^{o}C) to prevent oxidation. Once transported to the University of Saskatchewan, samples were stored in a N_2-filled glove box. Samples were not exposed to air until the XANES measurements were performed, which was approximately one year after the samples were collected from the TMF. A complete sample list, including sample elevation and aqueous Mo pore water concentration, is found in Supporting Information (Table S1). The concentrations of select elements in the tailings solids, as determined by ICP-MS, are also found in Supporting Information (Table S2).

Mo K-edge XANES

All Mo K-edge XANES measurements were performed using the Hard X-ray MicroAnalysis (HXMA) beamline (06ID-1) at the Canadian Light Source.[8] Samples were packed into 2.33 mm thick rectangular Teflon holders, which were sealed with two layers of Kapton tape. Samples were positioned in front of the X-ray beam at a 45^{o} angle. Spectra were collected from 19800–20650 eV with a step size of 0.3 eV near the Mo K-edge. The energy range was selected using a silicon (220) crystal monochromator that provided a monochromatic flux on the order 10^{12} photons/sec with a resolution of 2 eV at 20 keV, which is less than the natural linewidth of the Mo K-edge (4.52 eV).[9] All spectra were measured in partial fluorescence yield (PFY) mode using a 32 element Ge detector and calibrated against Mo metal, with the maximum of the first derivative of the Mo K-edge set to 20,000 eV.[10] Multiple scans were collected for each spectrum. The samples were observed to not undergo any X-ray beam-induced reduction as there was no change in the spectra between successive scans.

All XANES spectra were analysed using the Athena software program.[10] A quantitative analysis of the spectra was conducted by performing a principal component analysis (PCA)

followed by a linear combination fitting (LCF) of the spectra. The energy range used for the PCA and LCF analysis was 19990–20075 eV. The standards used in the LCF analysis (MoS_2, MoO_2, MoO_3, H_2MoO_4, $CaMoO_4$, α-$NiMoO_4$, α-$FeMoO_4$, $Fe_2(MoO_4)_3 \bullet 8H_2O$, $Fe(OH)_3$ – MoO_4.) were the same as those used in our previous Mo K-edge XANES study.[7] An energy shift was not applied during the LCF as the standards were calibrated against the same reference (Mo metal) as the tailings samples.

Results and Discussion

Mo K-edge XANES spectra

The Mo K-edge XANES spectra of representative tailings samples from the central and peripheral bore holes are shown in Figure 1. The complete set of Mo K-edge XANES spectra from the tailings samples studied can be found in the Supporting Information (Figures S1 – S2). The Mo K-edge corresponds to the dipole-allowed ($\Delta l = \pm 1$) transition of the 1s electron into unoccupied Mo 5p states. In general, the absorption edge energy is sensitive to the oxidation state of Mo, as well as bond covalency.[7,11] A low intensity pre-edge feature (19990–20010 eV) is also observed in the Mo K-edge, which corresponds to a dipole-forbidden ($\Delta l = \pm 2$) transition of a 1s electron into unoccupied Mo 4d states. The intensity of the pre-edge is influenced by the local coordination environment of the absorbing Mo atom.[11]

The majority of the Mo K-edge XANES spectra from the tailings samples have similar lineshapes. The Mo K-edge absorption-edge energy (and general lineshape) of the tailings samples were more similar to that of MoO_3 (Mo^{6+}) than MoO_2 or MoS_2 (Mo^{4+}), as shown in Figure 2. The Mo K-edge lineshape of the tailings samples are also different than that of tetrathiomolybdate ($[MoS_4]^{2-}$; Mo^{6+}),[12] indicating that the tailings samples consist mostly of Mo^{6+} oxides, which is in agreement with a previous report.[7] Broadening of the near-edge region

of spectra from samples collected from the central bore hole (Figure 1a) was observed, which may be due to the presence of Mo^{4+}.[13,14]

Principle Component Analysis

Visual inspection of the Mo K-edge XANES spectra suggests the tailings consist of multiple Mo species. Advanced analysis techniques are required to identify and quantify the Mo-bearing species in the TMF. Principle component analysis (PCA) was first used to determine the number of Mo species present in the 2013 tailings samples. The PCA calculation decomposes a series of spectra into a set of components that describes the variation in the data set.[15,16] Full details of the PCA analysis can be found elsewhere.[7] Results of the PCA analysis for samples from each bore hole can be found in the Supporting Information (Figure S3). The IND function, an empirical function used to differentiate between major and minor components in a PCA, was calculated for each bore hole to determine the minimum number of components in each series.[17,18] It is generally accepted that the minimum number of components is given when the IND function is minimized.[17,18] The IND values are generally small after the first component, which may be due to variations in the number of species present in each sample. The similar IND values obtained for 2 – 4 components suggests a maximum of four components are present in the tailings samples. This can be observed when reconstructing the spectra from tailings samples TMF13-01-SA23 (see Figure S4 in the Supporting Information), where a slight improvement is observed (particularly in the pre-edge region) when reconstructing the spectrum with four components.

Linear Combination Fitting Analysis

Linear combination fitting (LCF) analysis was employed to identify the Mo species present in the tailings samples. Each normalized Mo K-edge spectrum was fitted to the linear

combination of weighted standard spectra. The Mo K-edge XANES spectra from the Mo-bearing standards used in the LCF analysis are plotted in Figure S5 in the Supporting Information. All of the Mo^{6+} standards consist of MoO_4 tetrahedral units; however, the Mo K-edge lineshape of these standards are quite different in the near-edge region (20010–20040 eV) due to effects from the presence of different next-nearest neighbours (i.e. Ca, Fe, etc). The coefficients calculated in the LCF, which correspond to the concentration of each Mo species relative to the total amount of Mo in the tailings, were allowed to vary between 0 and 1 with the total sum of the coefficients constrained to 1. Several different fitting models using different combinations of standards were tested. Best fits were determined by calculating the goodness-of-fit parameters (R-value and χ^2). Generally, the fit with the smallest R-value and χ^2 value was considered the best. Decreasing the fitting range from 19990–20075 eV to 19990–20040 eV had no effect on the calculated concentrations, indicating that there are sufficient details in the pre- and near-edge regions to distinguish between the different Mo species in the tailings samples. Results of the best fits are tabulated in Table 1 and representative fitted spectra are shown in Figure 3. The fitted spectra from all other tailings samples are presented in Figures S6 – S9 in the Supporting Information.

The best fits were obtained when fitting the spectra to ferrimolybdite ($Fe_2(MoO_4)_3*8H_2O$), powellite ($CaMoO_4$), molybdate adsorbed on ferrihydrite ($Fe(OH)_3$ – MoO_4), and molybdenite (MoS_2). The concentration of molybdenite is small in most tailings samples (less than 10 at%). However, including molybdenite significantly improves the fitting of the near-edge region and the goodness-of-fit (see Figure S10 and Table S3 in Supporting Information). This suggests that molybdenite is an essential component in the fittings. Because of the oxic conditions of the TMF, the likely source of molybdenite is unprocessed ore that was

not fully oxidized during the uranium milling process. Although molybdenite was not found in our previous XANES study of samples collected in 2008, it does not mean that molybdenite was not present in the TMF during this period.[7]

It should be noted that slightly better fits were obtained when using molybdic acid (H_2MoO_4) rather than powellite. However, molybdic acid is soluble at the pH of the TMF (~7-8).[19] As such, molybdic acid was excluded from the fittings. The overfitting of the broad peak near 20040-20060 eV is likely due to multiple scattering resonance (MSR) peaks contributing to the intensity of this feature. MSR is a low-energy extended X-ray absorption fine structure (EXAFS) phenomenon that is highly dependent on crystal structure and crystallinity.[20] The intensity of MSR contributions decreases with decreasing crystallinity, and the overfitting observed in this region is indicative of the poor crystallinity of these materials. This observation is consistent with our previous study of the 2008 tailings samples.[7]

Comparison of the Mo speciation in the 2008 and 2013 tailings samples.

The Mo K-edge XANES spectra of the 2008 and 2013 tailings samples collected at the same depth were noticeably different (see Figure S11 in the Supporting Information). This suggests that changes in the Mo speciation in the tailings have occurred over the five year period between sampling campaigns. Comparing the relative amounts of Mo^{6+} species in tailings samples collected at different dates from the same elevation and bore hole can provide some indication as to which Mo^{6+} species are stable in the TMF over long periods of time. In 2008: the tailings deposited at approximately 411 mASL (meters above sea level) were less than a year old; at 398 mASL the tailings were approximately five years old; and at 371 mASL the tailings were approximately ten years old. It follows for the 2013 samples that the tailings sampled at 411, 398, and 371 mASL are approximately five, ten, and fifteen years old, respectively. Figure

4 compares the distribution of Mo^{6+} species from the peripheral bore hole in 2008 and 2013. Near the surface of the TMF (~411 mASL), the relative amount of powellite increased from 10 at% (2008 tailings sample) to 25 at% (2013 tailings sample). In contrast, the relative amounts of ferrimolybdite and molybdate adsorbed on ferrihydrite decreased over the same five year period, suggesting that powellite is more stable in the TMF over time. Smaller changes in the amount of powellite present were observed at lower elevations. It is apparent that relatively rapid changes in the Mo mineralogy occurs within the first five years of placement in the TMF. Following this, the precipitation of powellite appears to slow at lower elevations.

Depth analysis of the TMF

Powellite precipitates over time in the TMF, which is consistent with the predicted geochemical model (equation 1). This can be confirmed by comparing the relative amounts of solid Mo species in the TMF to the aqueous Mo pore water concentration. The aqueous Mo pore water concentration is plotted against the sample elevation for the central and peripheral bore holes in Figure 5. In general, higher aqueous Mo pore water concentrations are observed at elevations above 400 mASL (i.e. closer to the surface of the TMF) and sharply decrease at lower elevations. This suggests that, within the older tailings, a solid Mo mineral phase forms that results in a decrease of the aqueous Mo pore water concentration. It should be noted that this effect is more evident in the peripheral bore hole compared to the central bore hole.

As shown in Figure 5a, a sharp increase in the relative amount of powellite in the tailings is observed at elevations below ~400 mASL, particularly in the peripheral bore hole. The aqueous Mo pore water concentration remains low in tailings containing relatively high powellite content. The increase in the relative amount of powellite at lower elevations confirms that aqueous Mo precipitates to form powellite over time. The opposite trend is observed in the

223 combined relative amounts of ferrimolybdite and molybdate adsorbed on ferrihydrite (Figure
224 5b). Elevated concentrations of Mo in the pore water of the upper tailings are consistent with the
225 dissolution of ferrimolybdite and molybdate adsorbed on ferrihydrite. The dissolution and re-
226 precipitation of Mo as powellite confirms that the existing Mo geochemical model of the TMF is
227 correct and that powellite controls the long term stability of Mo in the pore water.

228 The effects of particle size of the tailings can be observed by comparing Mo speciation of
229 the tailings from the central bore hole compared to the peripheral bore hole. A larger amount of
230 molybdenite (~30 at%) is observed in three samples (TMF13-01-SA21, TMF13-01-SA22,
231 TMF13-01-SA23) collected from the central bore hole at 370 – 380 mASL. As shown in Figure
232 6a, the increase in molybdenite content correlates with a small increase in the aqueous Mo pore
233 water concentration at roughly the same elevation in the central bore hole. There is no
234 significant change in the amount of molybdenite or aqueous Mo pore water concentration of the
235 peripheral bore hole with increasing depth (Figure 6b). Under the conditions of the TMF,
236 molybdenite should oxidize. Therefore, the aqueous Mo pore water concentration should be
237 higher in regions of the TMF containing large (~30 at%) amounts of molybdenite, as is
238 illustrated in Figure 6a. Note that there was no correlation between the aqueous Mo pore water
239 concentration and the amount of molybdenite at elevations above 400 mALS. This is likely due
240 to the dissolution of ferrimolybdite and molybdate adsorbed on ferrihydrite at higher elevations,
241 increasing the levels of Mo in the pore water and masking this more minor effect.

242 Overall, these results show that the aqueous Mo pore water concentration decreases as a
243 direct result of the precipitation of powellite.

244

Acknowledgments

AREVA Resources Canada and the National Science and Engineering Research Council of Canada (NSERC), through a collaborative research and development grant, are thanked for funding this research. The authors would like to extend their thanks to Dr. Ning Chen and Dr. Weifeng Chen for their help in performing measurements on the HXMA beamline (06-ID1, CLS). The CLS is funded by NSERC, the Canadian Foundation of Innovation (CFI), the National Research Council (NRC), the Canadian Institutes of Health Research (CIHR), the Government of Saskatchewan, the Western Economic Diversification Canada, and the University of Saskatchewan. The Saskatchewan Research Council's Environmental Analytical Division, are thanked for performing ICP-MS measurements. M. R. Rafiuddin, E. Aluri, and A. Sarkar (University of Saskatchewan) and B. Schmid (AREVA Resources Canada) are thanked for their contributions.

Associated Information

Additional details of the Mo content of the tailings samples, results of the PCA of the tailings samples, fitted Mo K-edge spectra from additional tailings samples, and Mo K-edge XANES spectra comparing the 2008 and 2013 tailings samples are reported. This material is available free of charge via the Internet at http://pubs.acs.org.

References

1. Rowson, J.; Schmid, B. Validation of long term tailings performance report; AREVA Resources Canada: Saskatoon, Saskatchewan, Canada, **2009**. A copy of the report can be requested from AREVA Resources Canada (e-mail: publicrelations@areva.ca) or the Canadian Nuclear Safety Commission (http://nuclearsafety.gc.ca/eng/uranium/mines-and-mills/nuclear-facilities/mcclean-lake/index.cfm).

2. Langmuir, D.; Mahoney, J.; Rowson, J. Solubility products of amorphous ferric arsenate and crystalline scorodite ($FeAsO_4 \cdot 2H_2O$) and their application to arsenic behaviour in buried mine tailings. *Geochim. Cosmochim. Acta* **2006**, *70*, 2942−2956.

3. Mahoney, J.; Slaughter, M.; Langmuir, D.; Rowson, J. Control of As and Ni releases from a uranium mill tailings neutralization circuit: Solution chemistry, mineralogy and geochemical modeling of laboratory study results. *Appl. Geochem.* **2007**, *22*, 2758−2776.

4. Chen, N.; Jiang, D. T.; Cutler, J.; Kotzer, T.; Jia, Y. F.; Demopoulos, G. P.; Rowson, J. W. Structural characterization of poorly-crystalline scorodite, iron(III)−arsenate co-precipitates and uranium mill neutralized raffinate solids using X-ray absorption fine structure spectroscopy. *Geochim. Cosmochim. Acta* **2009**, *73*, 3260−3276.

5. Essilfie-Dughan, J. E.; Pickering, I. J.; Hendry, M. J.; George G. N.; Kotzer, T. Molybdenum speciation in uranium mine tailings using X-ray absorption spectroscopy. *Environ. Sci. Technol.* **2011**, *45*, 455-460.

6. Mahoney, J. Review of the Molybdenum Geochemistry in the JEB TMF; AREVA Resources Canada: Saskatoon, Saskatchewan, Canada, **2010**.

7. Hayes, J. R.; Grosvenor, A. P.; Rowson, J.; Hughes, K.; Frey, R. A.; Reid, J. Analysis of the Mo Speciation in the JEB Tailings Management Facility at McClean Lake, Saskatchewan. *Environ. Sci. Technol.* **2014**, *48* 4460-4467.

8. Jiang, D. T.; Chen, N.; Zhang, L. Malgorzata, G.; Wright, G. XAFS at the Canadian Light Source. *AIP Conf. Proc.* **2007**, *882*, 893-895.

9. Krause, M. O.; Oliver, J.H. Natural widths of atomic K and L levels, K_α X-ray lines and several KLL Auger lines. *J. Phys. Chem. Ref. Data* **1979**, *8*, 329-338

10. Ravel, B.; Newville, M. ATHENA, ARTEMIS, HEPHAESTUS: data analysis for X-ray absorption spectroscopy using IFEFFIT. *J. Synchrotron Rad.* **2005**, *12*, 537-541.

11. Farges, F.; Siewert, R.; Brown, G. E.; Guesdon, A.; Morin, G. Structural environments around molybdenum in silicate glasses and melts. I. Influence of composition and oxygen fugacity on the local structure of molybdenum *Can. Mineral.* **2006**, *44*, 731-753.

12. Dahl. T. W.; Chappaz, A.; Fitts, J. P.; Lyons, T. W. Molybdenum reduction in a sulfide lake: Evidence from X-ray absorption fine-structure spectroscopy and implications for the Mo Paleoproxy. *Geochim. Cosmochim. Acta* **2013**, *103,* 213-231.

13. Chen, K.; Xie, S.; Bell, A. T.; Iglesia, E Structure and properties of oxidative dehydrogenation catalysts based on MoO_3/Al_2O_3. *J. Catal.* **2001**, *198*, 232-242.

14. Zhai, Z.; Getsoian, A. Bell, A. T. The kinetics of selective oxidation of propene on bismuth vanadium molybdenum catalysts. *J. Catal.* **2013**, *308*, 25-36.

15. Fernández-Garcìa, M.; Márquez Alvarez, C.; Haller, G.L. XANES-TPR study of Cu – Pd bimetallic catalysts: application of factor analysis. *J. Phys. Chem.* **1995**, *99*, 12565–12569.

16. Beauchemin, S.; Hesterberg, D.; Beauchemin, M. Principal component analysis approach for modelling sulphur K-XANES spectra of humic acids. *Soil Sci. Soc. Am. J.* **2002**, *66*, 83-91.

17. E.R. Malinowski, Factor Analysis in Chemistry, 3rd ed., John Wiley & Sons, New York, 2002.

18. Malinowski, E.R. Theory of error in factor analysis. *Anal. Chem.* **1977**, *49*, 606-612.

19. Frey, R. Personal communication; AREVA Resources Canada: Saskatoon, Saskatchewan, Canada, **2013**.

20. Rehr, J. J. Theoretical approaches to X-ray absorption fine structure Re. Mod. Phys. **2000**, *72*, 621-654.

313 **Figure Captions**

314 **Figure 1.** Representative Mo K-edge XANES spectra of tailings samples collected from the a)
315 central (TMF13-01) and b) peripheral (TMF13-03) bore holes.

316 **Figure 2.** The Mo K-edge XANES spectrum of tailings sample TMF13-01-SA23. The
317 absorption-edge energy is similar to that of MoO_3, suggesting a large concentration of Mo^{6+}.

318 **Figure 3.** The fitted Mo K-edge XANES spectra of tailings samples a) TMF13-01-SA01, b)
319 TMF13-01-SA22, c) TMF13-03-SA02, and d) TMF13-03-SA21. The linear combination fit of
320 the spectrum is shown in red and the residual is shown in green. The weighted spectra of the
321 standards used to the fit the spectra are also shown.

322 **Figure 4.** A comparison of the distribution of Mo^{6+} species (powellite, ferrimolybdite, and
323 molybdate adsorbed on ferrihydrite) from tailings samples collected from the peripheral bore
324 hole in 2008 and 2013. Note that a larger amount of powellite was observed in the 2013 tailings
325 samples, particularly at lower elevations.

326 **Figure 5.** The aqueous Mo pore water concentration (black line; ●) compared to the relative
327 amounts of solid a) powellite (red line; ■) and b) ferrimolybdite and molybdate adsorbed on
328 ferrihydrite (blue line; ▲) plotted against the sample depth of the central bore hole (left side) and
329 peripheral bore hole (right side). Errors in the Mo pore water concentrations are estimated to be
330 15% for concentrations greater than 1 mg/L. Where not apparent, the error bars are smaller than
331 the symbols.

332 **Figure 6.** The aqueous Mo pore water concentration (black line; ●) compared to the relative
333 amount of solid molybdenite (green line; ♦) plotted against the sample depth of the a) central
334 bore hole (TMF13-01) and b) peripheral bore hole (TMF13-03). The plots highlight the changes
335 in the aqueous Mo pore water concentration and sediment molybdenite at elevations below 400

336 m (i.e. older tailing samples). Errors in the Mo pore water concentrations are estimated to be
337 15% for concentrations greater than 1 mg/L. Where not apparent, the error bars are smaller than
338 the symbols.

Tables and Figures

Table 1. Results of the LCF analysis of the Mo K-edge XANES spectra from the tailings samples. Calculated errors are shown in brackets.

Sample	$CaMoO_4$ (at%)	$Fe(OH)_3$-MoO_4 (at%)	$Fe_2(MoO_4)_3$ (at%)	MoS_2 (at%)	R-factor	χ^2
TMF13-01-SA01	8(3)	43(2)	43(3)	7(5)	0.00276	0.0592
TMF13-01-SA03	0(3)	55(3)	36(3)	9(5)	0.00306	0.0790
TMF13-01-SA04	18(3)	17(3)	41(4)	24(6)	0.00400	0.0932
TMF13-01-SA06	7(4)	63(3)	20(4)	10(6)	0.00415	0.115
TMF13-01-SA11	41(2)	30(2)	11(3)	19(4)	0.00181	0.0470
TMF13-01-SA12	38(2)	37(2)	17.4(6)	8(4)	0.00230	0.0519
TMF13-01-SA14	20(3)	55(2)	7(3)	17(5)	0.00304	0.0747
TMF13-01-SA19	30(2)	41(2)	13(3)	16(4)	0.00185	0.0466
TMF13-01-SA20	16(3)	45(3)	28(4)	11(6)	0.00400	0.102
TMF13-01-SA21	12(4)	54(5)	5(3)	29.7(9)	0.00450	0.113
TMF13-01-SA22	27(2)	42(2)	3(3)	28(4)	0.00196	0.0489
TMF13-01-SA23	10(3)	59(3)	4(3)	27(5)	0.00306	0.0778
TMF13-01-SA24	30(3)	24(3)	31(3)	16(5)	0.00319	0.0855
TMF13-01-SA25	19(3)	42(3)	25(4)	14(6)	0.00417	0.102
TMF13-03-SA02	5(3)	51(3)	36(3)	8(5)	0.00281	0.0742
TMF13-03-SA04	4(3)	26(3)	60(4)	10(6)	0.00391	0.0974
TMF13-03-SA06	25(2)	43(2)	25(3)	9(4)	0.00195	0.0508
TMF13-03-SA07	6(1)	51(1)	37(2)	6(3)	0.000993	0.0247
TMF13-03-SA11		85(4)		15(9)	0.00871	0.239
TMF13-03-SA12	44(3)	32(3)	16(3)	8(5)	0.00269	0.0732
TMF13-03-SA14	31(3)	19(3)	38(3)	13(5)	0.00335	0.0866
TMF13-03-SA15	39(3)	20(2)	26(3)	14(5)	0.00282	0.0709
TMF13-03-SA19	40(3)	30(2)	23(3)	7(4)	0.00214	0.0565
TMF13-03-SA21	45(3)	19(3)	22(4)	15(6)	0.00406	0.103
TMF13-03-SA22	38(3)	28(3)	26(3)	9(5)	0.00286	0.0750

Figure 1

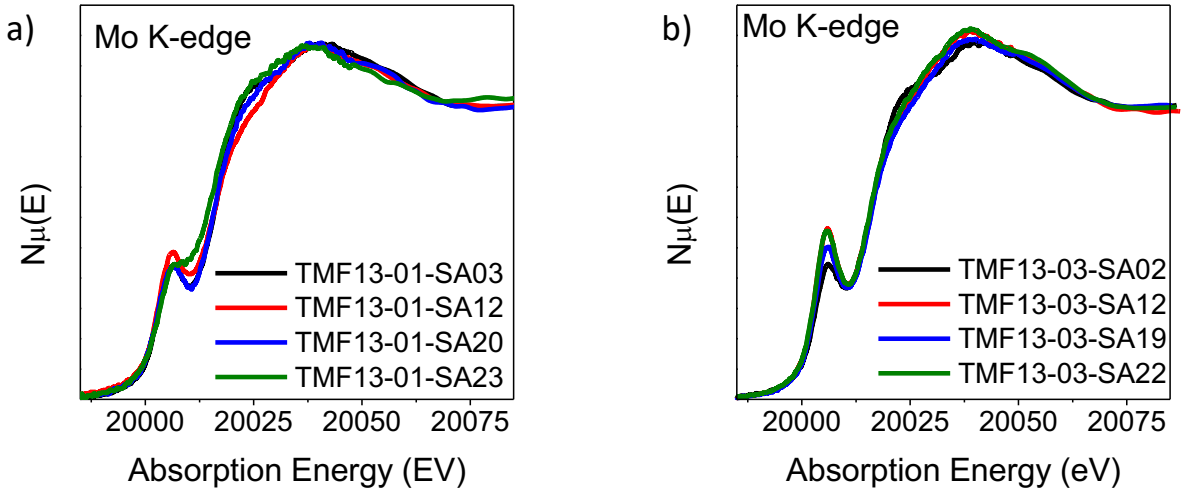
a)
Mo K-edge
Nμ(E)
TMF13-01-SA03
TMF13-01-SA12
TMF13-01-SA20
TMF13-01-SA23
20000
20025
20050
20075
Absorption Energy (EV)
b)
Mo K-edge
Nμ(E)
TMF13-03-SA02
TMF13-03-SA12
TMF13-03-SA19
TMF13-03-SA22
20000
20025
20050
20075
Absorption Energy (eV)

Figure 2

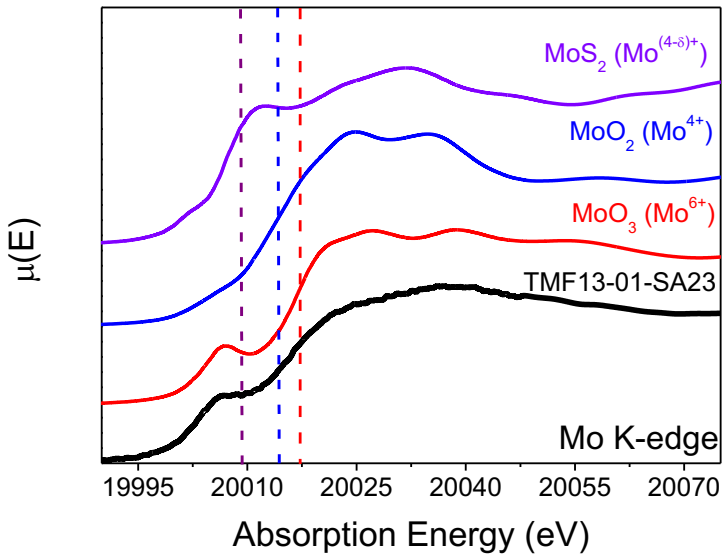
MoS2 (Mo(4-δ)+)
MoO2 (Mo4+)
MoO3 (Mo6+)
TMF13-01-SA23
Mo K-edge
μ(E)
19995
20010
20025
20040
20055
20070
Absorption Energy (eV)

Figure 3

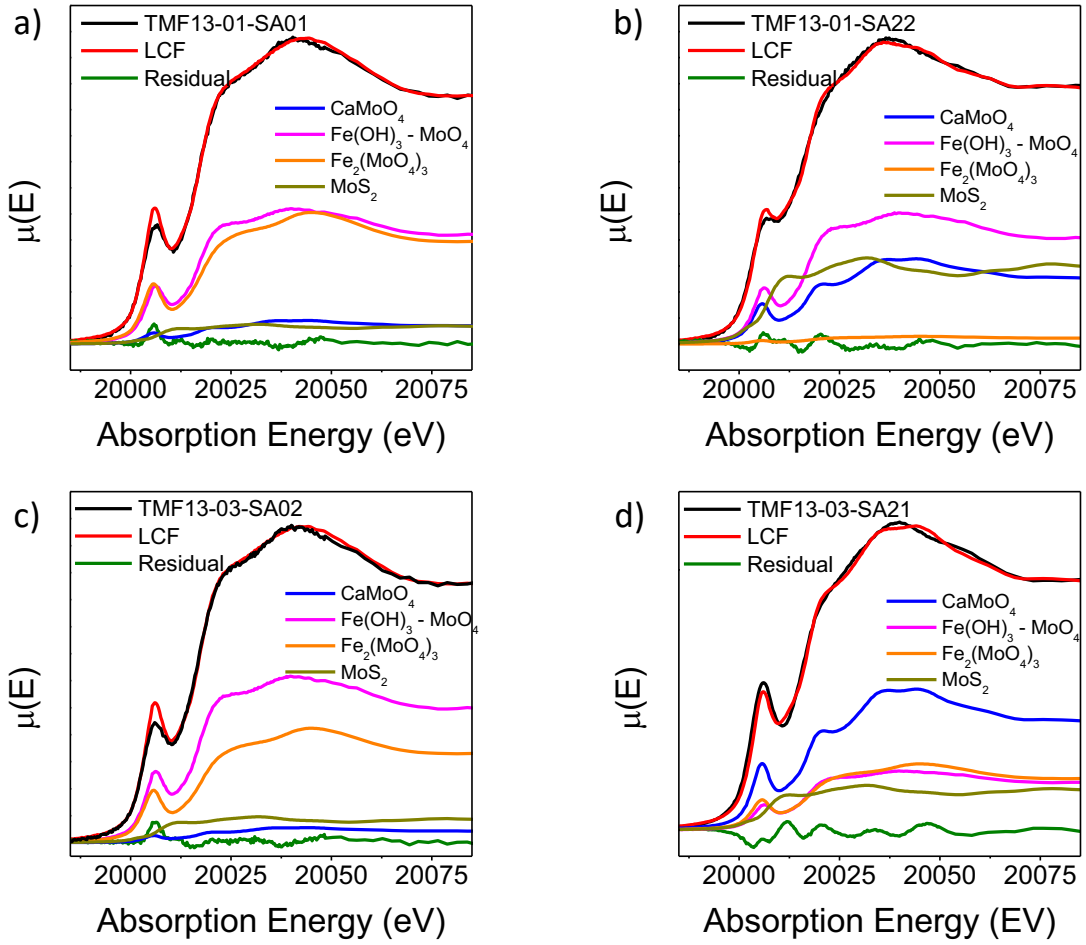
a)
TMF13-01-SA01
LCF
Residual
CaMoO4
Fe(OH)3 - MoO4
Fe2(MoO4)3
MoS2
μ(E)
20000
20025
20050
20075
Absorption Energy (eV)
b)
TMF13-01-SA22
LCF
Residual
CaMoO4
Fe(OH)3 - MoO4
Fe2(MoO4)3
MoS2
μ(E)
20000
20025
20050
20075
Absorption Energy (eV)
c)
TMF13-03-SA02
LCF
Residual
CaMoO4
Fe(OH)3 - MoO4
Fe2(MoO4)3
MoS2
μ(E)
20000
20025
20050
20075
Absorption Energy (eV)
d)
TMF13-03-SA21
LCF
Residual
CaMoO4
Fe(OH)3 - MoO4
Fe2(MoO4)3
MoS2
μ(E)
20000
20025
20050
20075
Absorption Energy (EV)

Figure 4

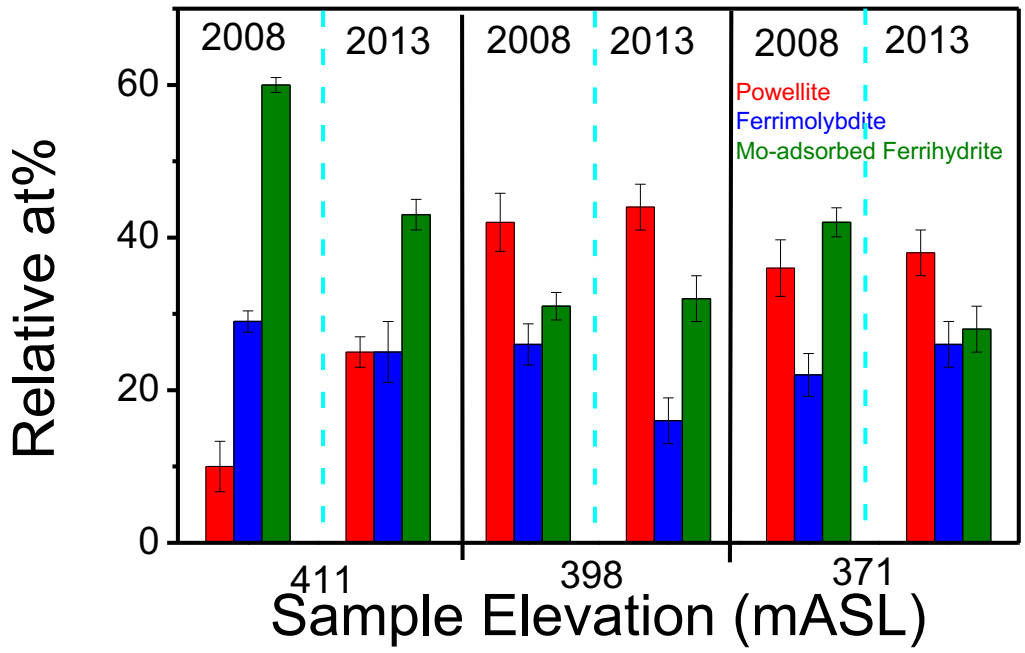
2008
2013
2008
2013
2008
2013
Powellite
Ferrimolybdite
Mo-adsorbed Ferrihydrite
Relative at%
60
40
20
0
411
398
371
Sample Elevation (mASL)

Figure 5

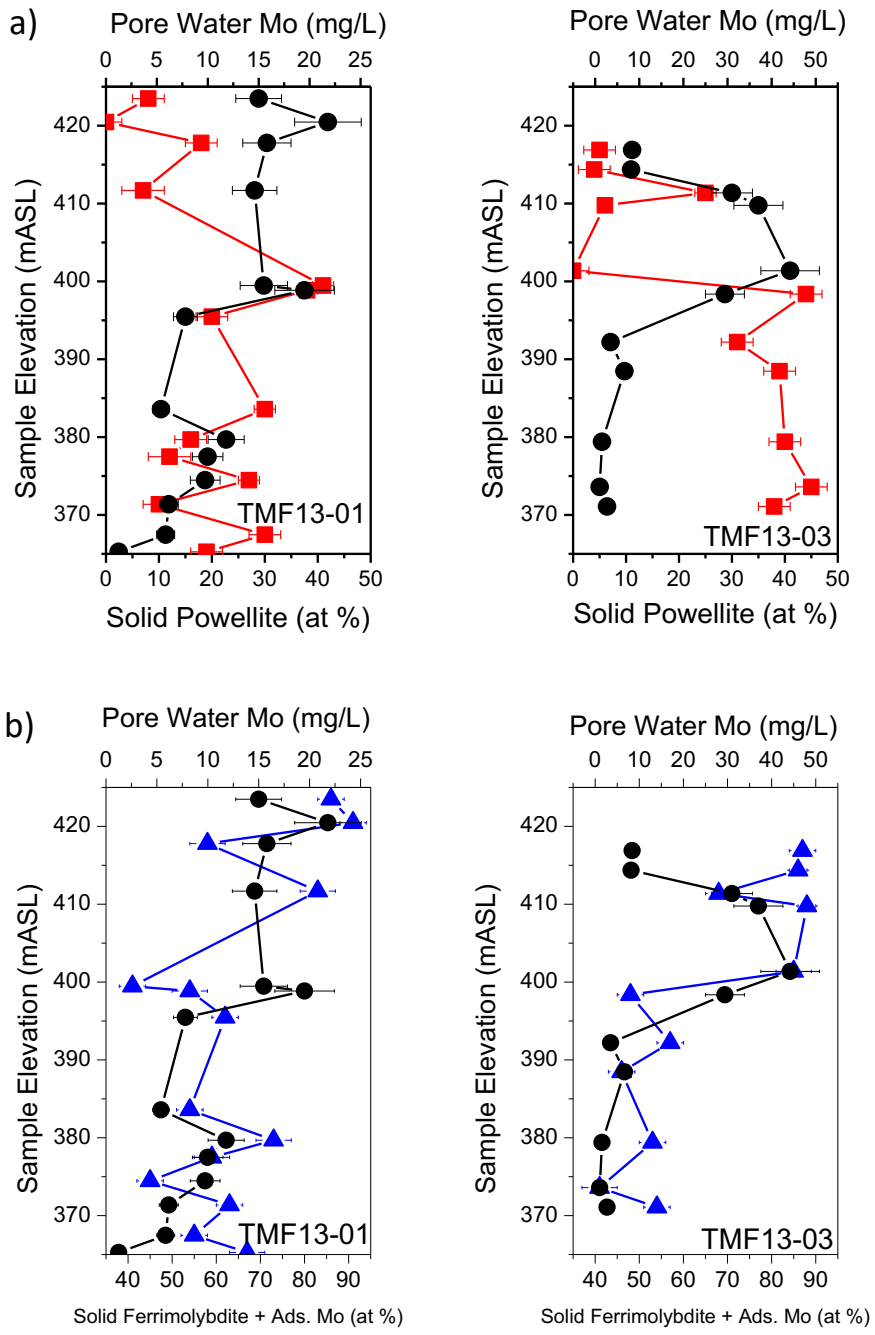
a)
Pore Water Mo (mg/L)
Sample Elevation (mASL)
Solid Powellite (at %)
TMF13-01
TMF13-03
b)
Solid Ferrimolybdite + Ads. Mo (at %)

Figure 6

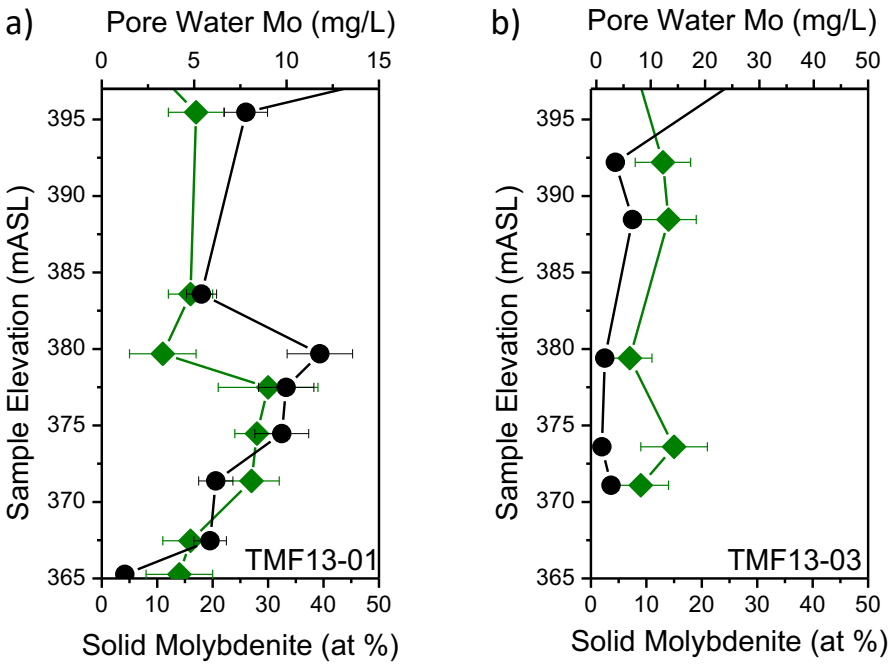
a)
Pore Water Mo (mg/L)
0
5
10
15
395
390
385
380
375
370
365
Sample Elevation (mASL)
TMF13-01
0
10
20
30
40
50
Solid Molybdenite (at %)
b)
Pore Water Mo (mg/L)
0
10
20
30
40
50
395
390
385
380
375
370
365
Sample Elevation (mASL)
TMF13-03
0
10
20
30
40
50
Solid Molybdenite (at %)

TOC Graphic

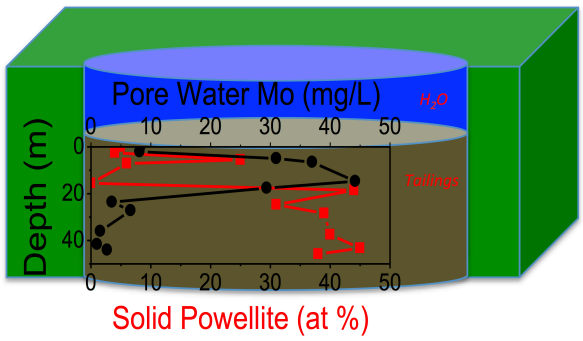
Pore Water Mo (mg/L)
H_2O
Depth (m)
0
10
20
30
40
50
0
20
40
Tailings
Solid Powellite (at %)